Integrins regulate GTP-Rac localized effector interactions through dissociation of Rho-GDI

Miguel Angel Del Pozo*†‡, William B. Kiosses*†, Nazilla B. Alderson*†, Nahum Meller*†, Klaus M. Hahn†, and Martin Alexander Schwartz*†§

**Division of Vascular Biology, †Department of Cell Biology, The Scripps Research Institute, 10550 N. Torrey Pines Road, La Jolla, California 92037, USA*
e-mail: ‡mdelpozo@scripps.edu or §schwartz@scripps.edu

Published online: 25 February 2002, DOI:10.1038/ncb759

The proper function of Rho GTPases requires precise spatial and temporal regulation of effector interactions. Integrin-mediated cell adhesion modulates the interaction of GTP-Rac with its effectors by controlling GTP-Rac membrane targeting. Here, we show that the translocation of GTP-Rac to membranes is independent of effector interactions, but instead requires the polybasic sequence near the carboxyl terminus. Cdc42 also requires integrin-mediated adhesion for translocation to membranes. A recently developed fluorescence resonance energy transfer (FRET)-based assay yields the surprising result that, despite its uniform distribution, the interaction of activated V12-Rac with a soluble, cytoplasmic effector domain is enhanced at specific regions near cell edges and is induced locally by integrin stimulation. This enhancement requires Rac membrane targeting. We show that Rho-GDI, which associates with cytoplasmic GTP-Rac, blocks effector binding. Release of Rho-GDI after membrane translocation allows Rac to bind to effectors. Thus, Rho-GDI confers spatially restricted regulation of Rac–effector interactions.

Spatial and temporal coordination between cell substrate adhesion and actin reorganization is essential for the protrusive activity that occurs at the leading edge during cell migration[1]. Actin organization is regulated by Rho family of low molecular weight GTPases and functions to extend the cell front, forming processes called filopodia and lamellipodia[2,3]. The binding of Rho GTPases to effector proteins regulates actin reorganization, in addition to other crucial biological events, such as gene expression and cell growth[4]. Interactions with effectors occur only when the GTPase is in the GTP-bound form, a state that is tightly regulated by guanine nucleotide exchange factors (GEFs) which stimulate GTP loading, GTPase activating proteins (GAPs) which catalyse GTP hydrolysis, and guanine nucleotide dissociation inhibitors (GDIs) which antagonize both GEFs and GAPs[5].

Rho-GDIs also mediate the cycling of Rho proteins between the cytosol and the membrane. Rho proteins contain a conserved CAAX sequence at their C termini, which is post-translationally modified by isoprenylation (through the addition of a geranyl geranyl moiety in the case of RhoA, Rac1 and Cdc42) of the cysteine residue[6]. The isoprenoid moiety is inserted into the lipid bilayer, anchoring the Rho protein to the membrane. Rho-GDIs form complexes with Rho GTPases in the cytoplasm, keeping them soluble by shielding the hydrophobic isoprenoid moiety[5,7]. Rho-GDIs therefore regulate both the GDP/GTP exchange cycle and the membrane association/dissociation cycle.

We recently identified a critical function for integrins in the membrane association of Rac[8]. Independent of their effects on GTP loading, integrins control the translocation of Rac to the plasma membrane. Growth factors can still activate Rac in non-adherent cells, but they do not show stimulation of Rac-downstream signalling events because of a failure of GTP-Rac to translocate to membranes. Membrane localization of Rac is required for the activation of its effector, Pak, and GTP-Rac binds with higher affinity to membranes from adherent cells relative to suspended cells. Therefore, integrins regulate the ability of Rac to couple with Pak through an effect on membrane binding sites for Rac[8,9]. In this manuscript, we investigated the importance of Rac–effector binding for integrin-mediated membrane translocation. While studying Rac activation and localization with a FRET assay[10], we made the unexpected observation that in spite of its homogeneous distribution throughout the cell, constitutively active Rac interacts with effectors selectively within specific regions at cell edges. Further analysis revealed that integrins induce local Rac–effector coupling by directing Rac to membranes and dissociating it from Rho-GDI. The data therefore define a new mechanism for the spatial control of Rac signalling, as well as a new function for Rho-GDI in preventing activation of Rac downstream cascades in the cytoplasm by blocking effector binding.

Results

Requirements for Rac membrane targeting. Why Rho family GTPases require GTP-loading to translocate to membranes is unclear. Some Rac effector proteins, such as Pak, also associate with membranes after cell activation[11]. We therefore sought to test whether effector binding was required for membrane translocation. To do this, we used a series of Rac effector loop mutants that also bear the GTPase-deficient Q61L mutation, which locks Rac in the 'active' GTP-bound state. The Y40C mutant is unable to bind to CRIB (Cdc42/Rac interactive binding)-sequence-containing Rac effectors such as Pak. The F37A mutant does not bind to the effectors POR-1 or p160ROCK, and the T35S mutation prevents binding to any of the known Rac effectors[12,13]. After transient expression in NIH-3T3 fibroblasts and cell fractionation, all of these mutant proteins were detected in the membrane fraction of adherent cells (Fig. 1a), suggesting that effector binding is not required for membrane localization. Rac that was cotransfected with Rho-GDI behaved similarly (data not shown). As a complementary approach, V12-Rac was expressed together with the p21-binding domain (PBD) of Pak, which competes with endogenous, membrane-bound effectors[14]. Subcellular

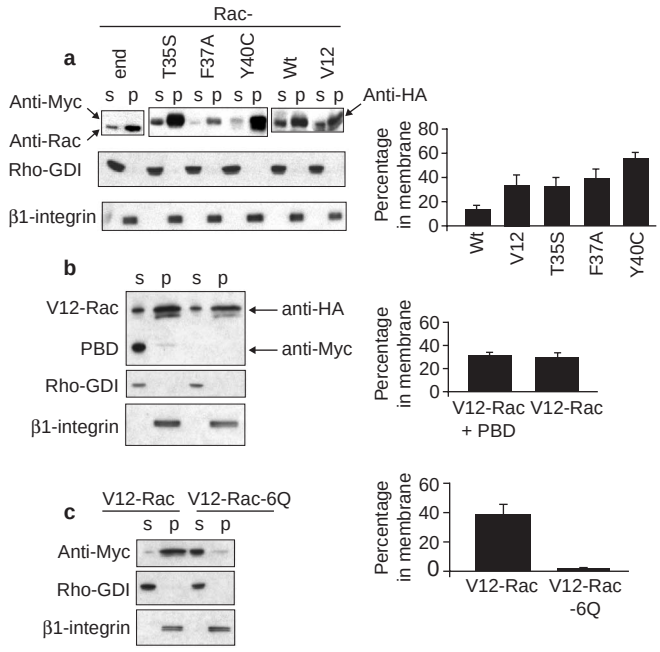

Figure 1 **Rac membrane targeting is independent of effector interactions but requires the C-terminal polybasic sequence. a**, NIH-3T3 cells were transiently transfected with empty control vector or Rac mutants, as indicated. After 24 h, cells were transferred to medium containing 0.2% serum. After 48 h cells, adherent cells were harvested and the particulate (p) and soluble (s) fractions were isolated (see Methods). Samples (10 μg protein) were analysed by SDS–polyacrylamide gel electrophoresis (PAGE) and western blotting with anti-Rac (endogenous protein, *end*), anti-Myc (Q61L–T35S-Rac, Q61L–F37A-Rac and Q61L–Y40C-Rac) or anti-HA (Wild type and V12-Rac) antibodies (left). The anti-integrin β1 subunit and anti-Rho-GDI were used as markers for the membrane and cytosol, respectively. Results are representative of four independent experiments. Note that the amount of protein analysed (10 μg per lane) represents 1–2% of the soluble fraction and 10–20% of the particulate fraction. Quantification of the membrane localization of the different Rac mutants is also shown (right). Data were normalized according to the total protein levels of each Rac mutant, and the percentage in the membrane fraction calculated. Values are means (SEM from four separate experiments). **b**, NIH-3T3 cells were cotransfected with HA–V12-Rac and either Myc–PBD or the empty vector, serum-starved for 24 h and then separated into particulate and soluble fractions for analysis as above. Quantification of HA–V12-Rac translocation to the membrane, as in **a**, is shown (right). Values are means (SEM from three independent experiments). **c**, Normal V12-Rac or V12-Rac with a mutated polybasic sequence in pRK5-myc were transiently transfected into NIH-3T3 cells and processed as above. Quantification of four independent experiments is also shown (right).

fractionation showed that V12-Rac binds to membranes independently of Pak-PBD expression (Fig. 1b). Immunofluorescence analysis performed in parallel verified that PBD efficiently blocked cell spreading, as previously described (data not shown)[14]. These results demonstrate that integrins regulate the membrane targeting of Rac independently of Rac effector binding.

Rac contains a polybasic region (KKRKRK) near the C terminus that is similar to a sequence in K-Ras, which is necessary for the association of K-Ras with the plasma membrane[15]. To test the relevance of this sequence for the membrane targeting of Rac, the effects of overexpression of a Rac mutant, in which the 6 basic residues were substituted by glutamine (V12-Rac-6Q), was examined. This mutant was less efficiently translocated to the membrane (Fig. 1c). Therefore, in addition to the isoprenyl group, the adjacent stretch of basic residues contributes to adhesion-dependent Rac membrane targeting. This result explains a previous report showing that this mutation almost completely abolished the ability of Rac to stimulate Pak activity[16].

Integrin regulation of Cdc42 membrane targeting. To test whether the effect of integrin on membrane targeting was exclusive to Rac, or was shared by its close relative Cdc42, NIH-3T3 fibroblasts were transfected with a construct in which green fluorescent protein (GFP) was fused to the amino terminus of wild-type Cdc42 (thus preserving its membrane-targeting CAAX sequence and the polybasic sequence). Adherent or suspended cells were stimulated with bradykinin, a specific Cdc42 agonist[17]. Confocal microscopy demonstrated that bradykinin induces the translocation of GFP–Cdc42 from the cytosol to membranes maximally at 20–30 min, in a strictly integrin-dependent manner (Fig. 2a). Interestingly, serial sections showed that Cdc42 was located primarily within the basal regions, near the occupied integrins; apical sections showed mainly cytoplasmic staining (Supplementary Information, Fig. S1). Subcellular fractionation confirmed that bradykinin induced the translocation of endogenous Cdc42 to the particulate fraction of adherent, but not suspended, cells (Fig. 2b). Thus Cdc42, like Rac, requires attachment to the extracellular matrix for growth-factor-induced membrane translocation.

Integrins regulate both the GTP-loading and the membrane targeting of these GTPases (Fig. 2a,b; see also ref. 8). To examine whether integrins are required for membrane targeting under conditions where GTP-loading (that is, activation) is constant, we used constitutively activated mutants of Rac and Cdc42 fused to GFP. Active Rac and Cdc42 were membrane associated only in adherent cells (Fig. 2c). Confocal analysis again demonstrated that activated Rac associates at the basal plasma membrane (Supplementary Information, Fig. S1); similarly, activated Cdc42 was also localized to the basal plasma membrane (data not shown). In cells that expressed GFP alone, no membrane localization was detected, whereas a GFP protein containing a myristylation membrane-targeting sequence was found in association with membranes under all conditions examined (Fig. 2c). As an additional control, we examined the localization of activated Rac and Cdc42 in cells, immediately after detachment. These cells clearly show membrane localization of Rac and Cdc42, and contrast with cells suspended for longer times (Fig. 2c). Analysis by subcellular fractionation yielded very similar results (Fig. 2d). To verify that integrins affect membrane targeting rather than GTP loading, we performed pull-down assays. These experiments confirmed that V12-Rac was equally loaded with GTP in both adherent and suspended cells (data not shown). Together, these data show that integrins regulate Rac and Cdc42 membrane translocation separately from their effects on GTP loading.

Enhancement of GTP-Rac coupling to effectors at regions of the cell edge. Complex functions, such as cell migration, involve the integration of multiple signalling networks that need to be spatially and temporally regulated within living cells[1,18,19]. An intriguing observation is that lamellipodia and filopodia are formed exclusively at the leading edge, where integrins establish contacts with the extracellular matrix[3,20]. It is possible that active/occupied integrins in the leading edge determine the spatial localization of these processes by targeting Rac and/or Cdc42 to these sites. In order to test this hypothesis, we measured localized Rac activation in single cells with an assay based on FRET between GFP-labelled Rac and Alexa-546-tagged PBD[10]. Binding of GFP–Rac to the Alexa–PBD, which occurs after Rac activation, results in FRET.

To study Rac targeting without any contribution from receptor-induced activation, we microinjected NIH-3T3 fibroblasts with a cDNA encoding GFP–V12-Rac. Staining with anti-Rac antibodies and quantification revealed that the protein levels of GFP–Rac were 1.51 (± 3.2 s.d., $n = 241$)-fold higher than the endogenous Rac. Both GFP–V12-Rac and the Alexa-labelled effector domain were distributed homogenously throughout the cell (Fig. 4a). The latter result is consistent with the almost exclusively cytoplasmic distribution of V12-Rac determined by subcellular biochemical fractionation

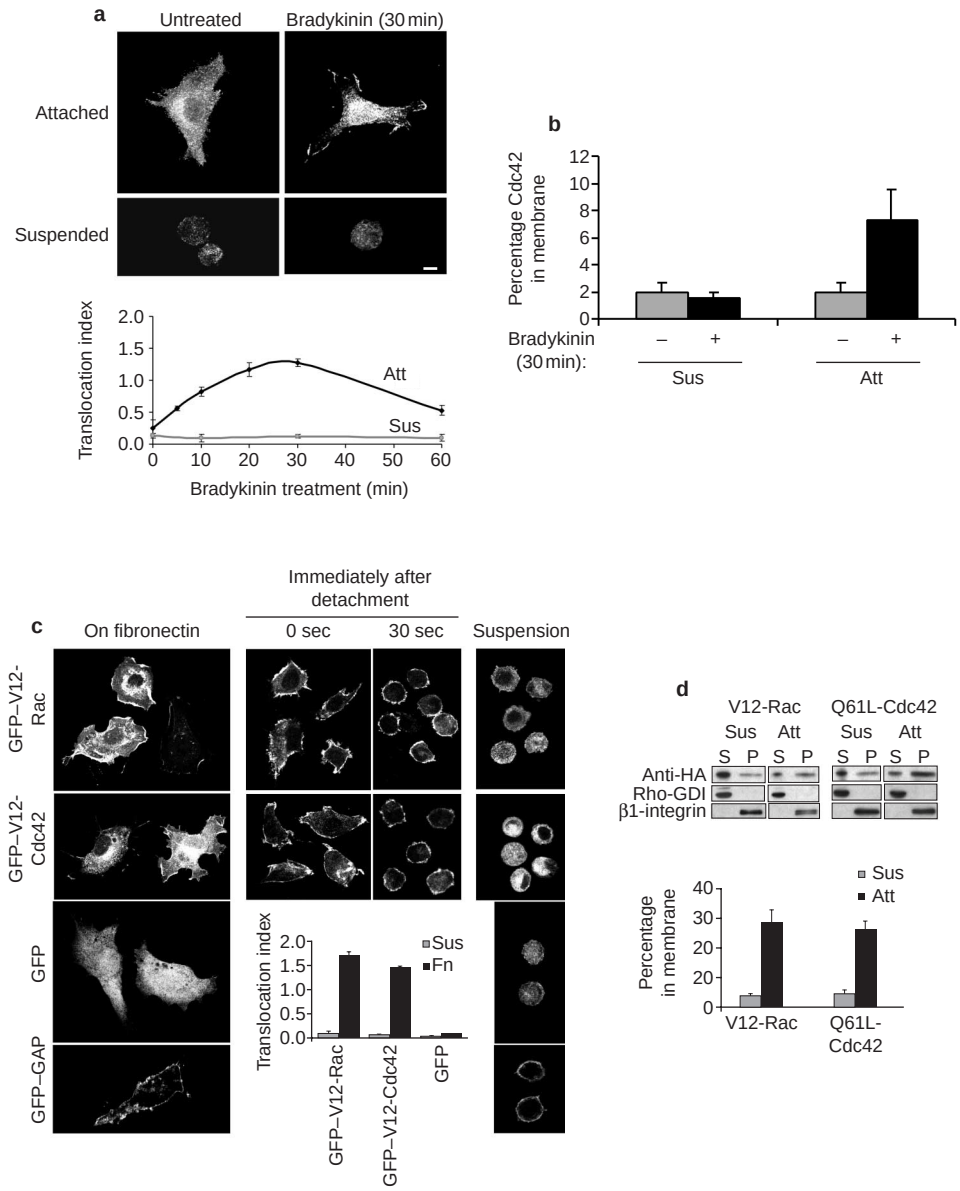

Figure 2 **Integrins regulate Cdc42 membrane targeting similarly to Rac.** **a**, NIH-3T3 were transiently transfected with GFP–Wt-Cdc42, serum starved for 24 h, replated on coverslips for 6 h or placed in suspension for 2 h before incubation in medium alone (untreated) or medium containing 100 ng ml^{-1} bradykinin for various times before fixation. Cells in suspension were then transferred to poly-L-lysine-coated coverslips, and all samples were analysed by confocal microscopy. Basal *z*-sections of cells in direct contact with the substrate are shown. The index of translocation to the plasma membrane was calculated (see Methods). Values are means (± SEM) from four independent experiments, in which more than 100 cells were scored for each condition. **b**, Serum-starved attached (Att) or suspended (Sus) cells were stimulated with 100 ng ml^{-1} bradykinin for 30 min at 37 °C and analysed by subcellular fractionation, western blotting with the anti-Cdc42 antibody and densitometric quantification. Values are means (SEM from four separate experiments). **c**, NIH-3T3 were transiently transfected with different GFP constructs, serum-starved for 24 h and plated onto fibronectin-coated coverslips or placed in suspension for 2 h before fixation. In some cases, cells were fixed immediately, or 30 sec after trypsin treatment. Immediately detached and suspended cells were then transferred to poly-L-lysine coverslips and samples processed as in **a**. The translocation index (showing means ± SEM from three independent experiments), in which more than 100 cells were scored per condition, is also shown (Inset). **d**, NIH-3T3 were transfected with 1.0 μg of total DNA containing 0.1 μg of Myc–Rho-GDI and 0.2 μg of active Rac or Cdc42. Cells were serum-starved and placed in suspension for 2 h, or kept stably adherent before subcellular fractionation and analysis by western blotting. Quantification of active Rac and Cdc42 translocation to the membrane (SEM from four independent experiments) is shown (right). Scale bar in **a** represents 10 μm, and also applies to **c**.

(Fig. 1b). The levels of injected Alexa–PBD did not inhibit lamellipodia formation (Figs 3 and 4; see also ref. 10). The uniform distribution of these proteins suggests that the FRET signal should also be uniform in the cell. Surprisingly, images showed that the level of the FRET signal was distinctly higher at regions of the cell edge (Fig. 3a). These areas generally appeared protrusive and very likely correspond to lamellipodia. As a negative control, we examined a GFP fusion of the Rac effector mutant Q61L–T35S, which is activated, but deficient in effector binding[12,13]. This mutant gave a low FRET signal that we take as a baseline. Notably, the level of this

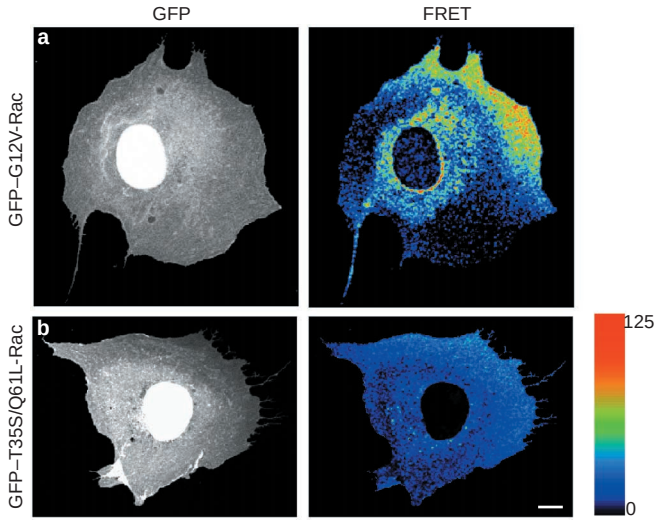

Figure 3 **FRET analysis demonstrates that GTP-Rac coupling to effectors is locally enhanced in lamellipodia.** NIH-3T3 cells were microinjected with cDNAs encoding the indicated GFP–Rac fusion proteins and then with Alexa–PBD protein. Representative GFP and corrected FRET images from three independent experiments are shown. A colour scale with the equivalent numerical values for the intensity of FRET for all images is displayed. Red represents a high FRET signal and blue, a low signal. Scale bar represents 10 μm.

signal was not increased in the leading edge (Fig. 3b), as observed with overexpression of V12-Rac. Thus, the efficiency of interaction between V12-Rac and a soluble effector domain is enhanced within the edges of spontaneously polarized cells.

Local effect of integrins on membrane targeting. In order to test the effect of local integrin stimulation on Rac coupling to effectors, we incubated cells with 5-μm beads coated with fibronectin, which induce localized occupancy and clustering of integrins[21,22]. As expected, the beads were able to induce the clustering of actin (data not shown). We also observed an increase in the level of the FRET signal around the bead (Fig. 4a). This signal approached maximal levels after an incubation of approximately 20–40 min with the beads (Supplementary Information Fig. S2) and was terminated after the beads were internalized at later times, as previously described[22]. In a fraction of cells, we noticed some accumulation of GFP–V12-Rac around the beads (for example, Fig. 4b), but this effect was not dramatic and was much less distinct than the FRET signal. Overexpression of the Q61L–T35S-Rac mutant resulted in little increase in FRET around the beads (14 ± 4%, $n = 45$ beads), in contrast to V12-Rac (84 ±8 %, $n = 55$). The effect was integrin-specific, as FRET was induced by beads coated with anti-β1 integrin antibodies, but only weakly with antibodies to a non-integrin cell surface adhesion receptor, such as CD44 (Fig. 4b). Quantification of three independent experiments demonstrated that 86 ± 9% of anti-β1-integrin-coated beads ($n = 25$), but only 14 ± 4% of anti-CD44-coated beads ($n = 38$), induced a positive FRET signal in cells expressing GFP–V12-Rac. Furthermore, for the small fraction of anti-CD44-coated beads that had positive signals, FRET intensity was 3.1 ± 0.2-fold lower than for anti-β1-integrin-coated beads. We also noticed that, unlike actin or cytoskeletal proteins[23], the FRET signal around fibronectin- or anti-integrin-coated beads was not always confined to the immediate vicinity of the bead. This result suggests that integrins may initiate signalling, but that propagation to nearby regions can also occur.

In order to confirm these results with a more physiological indicator, we performed FRET assays with wild-type GFP–Rac. In these experiments, overall FRET intensities were lower, but fibronectin-

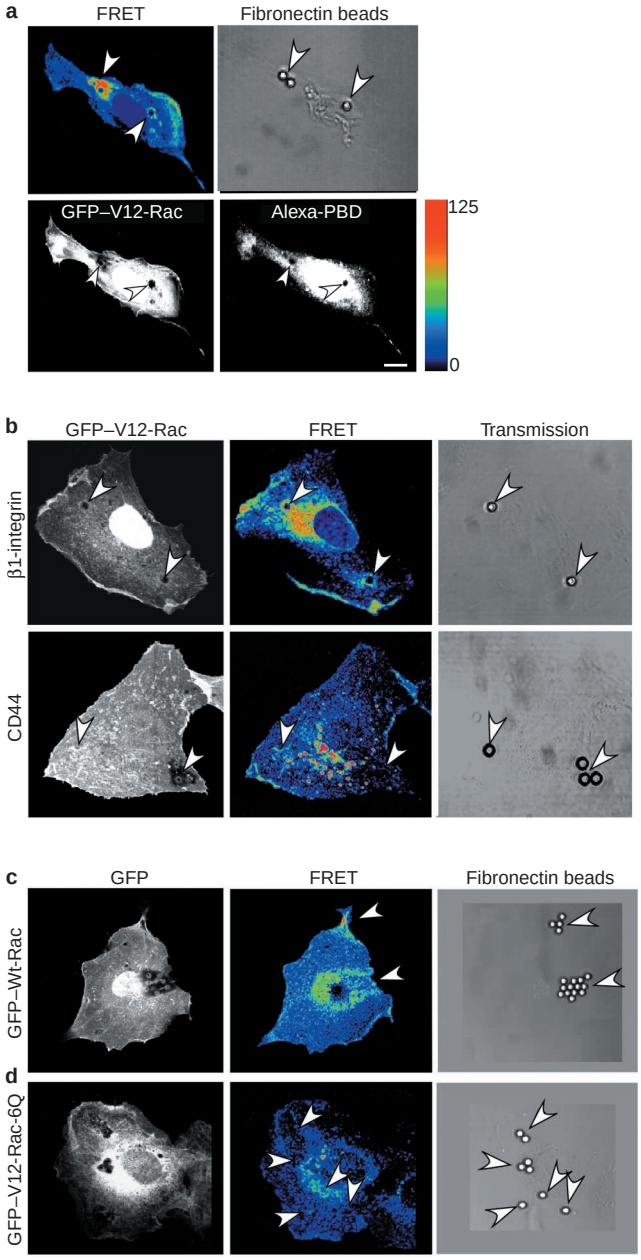

Figure 4 **GTP-Rac coupling to effectors is locally induced by integrin stimulation and requires Rac membrane targeting. a**, Cells expressing V12-Rac and Alexa–PBD were incubated for 20 min with 5-μm fibronectin-coated beads, shown in the phase-contrast image (upper right) and identified by arrowheads in other panels. Images of GFP (lower left) and Alexa (lower right) were recorded in fixed cells, corrected for background and bleed-through, to generate the corrected FRET image (upper left). The FRET intensity range for this figure is also shown (far right). **b**, Cells injected with GFP–V12-Rac and Alexa–PBD were incubated for 20 min with anti-β1-integrin-coated beads or anti-CD44 antibodies. GFP, corrected FRET and phase-contrast images are shown. **c**, **d**, Cells were injected with GFP–Wt-Rac (**c**) or a V12-Rac polybasic region mutant (**d**) and processed for FRET as above. Images are representative of three separate experiments. Scale bar represents 10 μm.

coated beads induced a positive FRET signal (Fig. 4c) and FRET was also higher at some edges and protrusions. Quantitative analysis showed that 66 ± 11% of fibronectin-coated beads ($n = 117$) and 69 ± 9% of anti-β1-coated beads ($n = 85$) induced a positive FRET

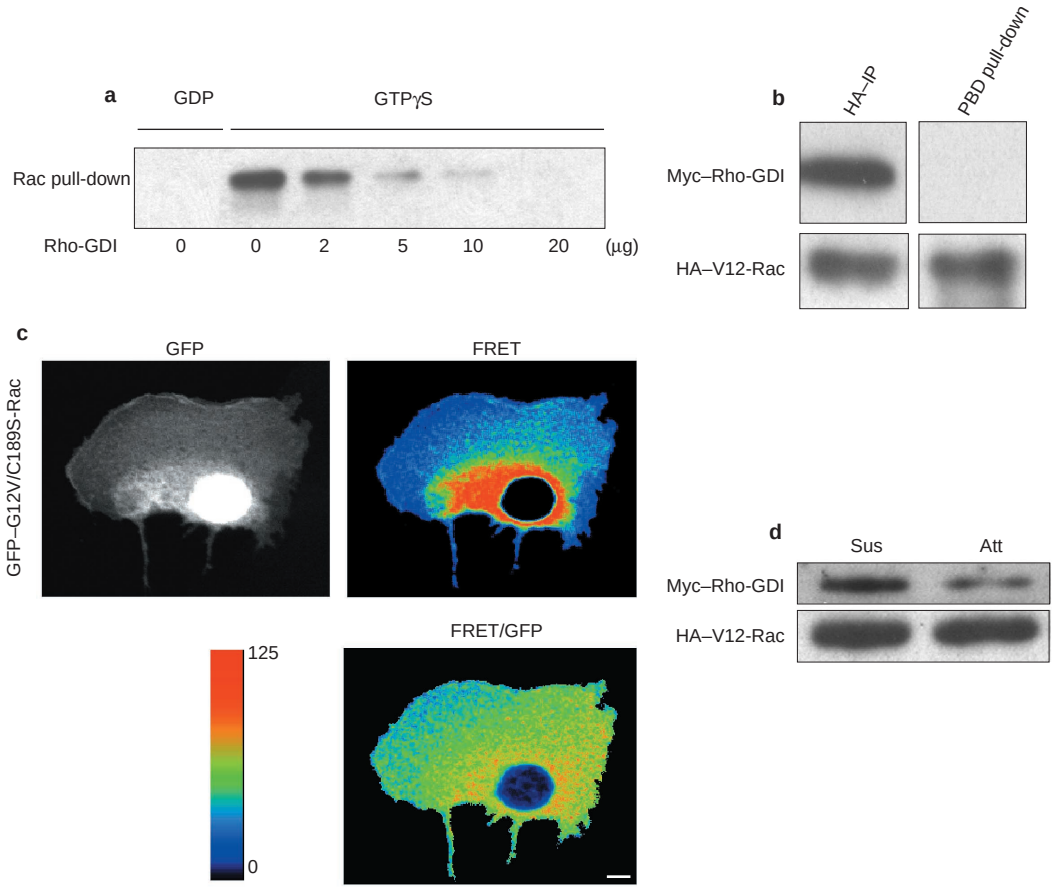

Figure 5 **Rho-GDI blocks GTP-Rac effector coupling. a**, Recombinant isoprenylated human Rac1 (0.5 μg per lane) was loaded with GDP or GTPγS and then incubated with 0–20 μg of recombinant purified human Rho-GDI for 30 min at 4 °C. The Rac protein was precipitated by incubation with 0.5 μg of recombinant human GST–PBD and detected by western blotting with an anti-Rac monoclonal antibody. Western blotting with an anti-GST monoclonal antibody demonstrated equivalent levels of PBD in each sample (data not shown). Results are representative of five independent experiments. **b**, NIH-3T3 were transfected with 1.0 μg of total DNA containing 0.1 μg of Myc–Rho-GDI and 0.2 μg of HA–V12-Rac. Cell lysates (200 μg of total cell protein per sample) were precipitated with either 0.5 μg of purified 12CA5 anti-HA monoclonal antibody or 10 μg of GST–PBD. Western blotting with the anti-Myc antibody identified exogenous Rho-GDI in the precipitates. Western blotting for V12-Rac demonstrates equivalent protein levels in each sample. Data are representative of three independent experiments. **c**, Cells were injected with a prenylation site V12-Rac mutant fused to GFP. Corrected FRET and FRET:GFP ratio images, which are representative of three independent experiments, are shown. Scale bar represents 10 μm. **d**, Cells were transfected as in **b**, serum-starved and then placed in suspension for 2 h, or kept stably adherent. Cell lysates were immunoprecipitated with the anti-HA monoclonal antibody and the Myc–Rho-GDI/HA–V12-Rac complex was detected by western blotting. Data are representative of three independent experiments.

signal with wild-type Rac. However, this result represents the effect of integrins on activation and targeting, whereas the effects on activated Rac mutants represent only targeting. Consistent with the activation of Rac by the hyaluronic acid receptor CD44 (ref. 24), we observed that anti-CD44-coated beads induced a weakly positive signal with GFP–Wt-Rac (35 ± 6%, $n = 88$). By contrast, beads coated with an antibody to the non-integrin fibronectin receptor syndecan-4 (ref. 25) had a negligible effect on GFP–Wt-Rac signal (8 ± 3%, $n = 64$).

To test whether these effects were related to Rac membrane localization, we examined a GFP fusion of the polybasic region mutant. This mutant is constitutively active because of the V12 mutation, although membrane targeting is reduced (Fig. 1c; results for the GFP fusion not shown). Fibronectin-coated beads induced a substantially lower FRET signal with this mutant (Fig. 4d). This result indicates that the increased FRET around the bead observed with GFP–V12-Rac (Fig. 4a) requires the targeting of Rac to membranes. The residual weak signal observed with GFP–V12-Rac-6Q is probably caused by the CAAX motif, which may mediate residual membrane association (Fig. 1c). This result demonstrates that membrane targeting is required for the binding of Rac to its effectors.

Rho-GDI blocks effector binding. Rho-GDIs regulate the membrane association/dissociation cycle of Rho GTPases. Structural studies of the complex between members of the GDI family and Rho family members have identified two important sites of interaction[26–29]. First, the geranyl geranyl moiety of the Rho protein is inserted into a hydrophobic pocket in GDI. Second, the N terminus of GDI binds to the switch-I and -II regions of the GTPase, which are also the binding sites for nucleotides, effectors, GAPs and GEFs. The binding of GDI inhibits both nucleotide exchange and GTP hydrolysis. GDI binds to Thr 35 in both Cdc42 and Rac2 (refs 26,27), which mutational studies have shown is an essential residue for effector binding[12,13].

In order to test whether Rho-GDI blocks effector binding, we measured the binding of recombinant isoprenylated Rac1 to the PBD effector domain of Pak, in the presence or absence of recombinant Rho-GDI. Increasing amounts of the Rho-GDI protein inhibited the binding of Rac1 to PBD, in a dose-dependent manner

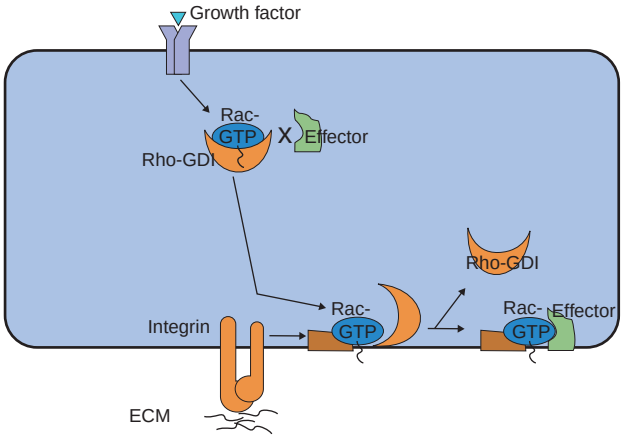

Figure 6 **Model for integrin-regulated localized enhancement of Rac membrane targeting and effector coupling.** Growth factors could increase Rac GTP-loading globally in the cell, but Rho-GDI would prevent GTP-Rac binding to effectors in the cytoplasm. Integrins would determine the specific local areas where Rac targets to membranes, leading to the dissociation of Rho-GDI.

(Fig. 5a). We also performed a complementary approach in living cells cotransfected with haemagglutinin (HA)-tagged V12-Rac and Myc-tagged Rho-GDI. As expected, V12-Rac immunoprecipitated through the HA tag was associated with GDI. However, when an equal amount of the activated Rac was precipitated through binding to the PBD, virtually no GDI was present, demonstrating that Rac cannot bind to both GDI and the effectors at the same time *in vivo* (Fig. 5b).

As Rac is only found in the cytosol when bound to GDI, this result could explain the failure of cytosolic V12-Rac to bind to its effectors. To test this idea, we examined the properties of a GFP fusion to V12-Rac, in which Cys 189 was mutated to Ser, to prevent prenylation. This mutant is constitutively active, but deficient in binding to both membranes and Rho-GDI. As expected, when assayed by fractionation, the construct was exclusively localized to the cytoplasm (data not shown). When examined with the fluorescence assay, the FRET signal was high and concentrated in the central thicker part of the cytoplasm. To confirm that the high FRET signal was caused by a greater volume in this region, we normalized the FRET signal to Rac concentration by dividing the FRET image by the GFP image. After normalization to the GFP signal, a more uniform level of FRET in the cytoplasm was evident (Fig. 5c). To confirm this effect, we calculated the average pixel intensities for the V12-Rac and V12-Rac-SAAX FRET signals over the entire cell. The average FRET/pixel intensities were 37.3 ± 13 for normal V12-Rac and 49.4 ± 27.7 for the V12/SAAX mutant (n = approximately 30). Taking V12/T35S as the baseline (average intensity = 28.7 ± 9.3), this result shows that the specific signal for the SAAX mutant was 2.4-fold higher than its prenylated counterpart. This result demonstrates that a Rac mutant that does not bind Rho-GDI shows high *in vivo* binding to the PBD. As expected, fibronectin-coated beads did not enhance the FRET signal with this mutant (9 ± 4%, n = 90). This result supports the idea that Rho-GDI prevents Rac coupling to effectors in the cytoplasm.

If integrins regulate GTP-Rac membrane targeting, they should modulate the association of V12-Rac with Rho-GDI. Co-immunoprecipitation experiments showed a decrease in the V12-Rac–Rho-GDI complex in adherent cells, as compared with cells in suspension (Fig. 5d; 1.81 ± 0.17-fold, n = 3). This result supports the concept that integrin-induced GTP-Rac membrane targeting is accompanied by the dissociation of Rho-GDI.

Discussion

We propose that growth factors can induce the global GTP loading of Rac and that under some conditions, GTP-Rac may be present in the cytosol[8], but that the binding of Rho-GDI will prevent GTP-Rac from coupling to cytoplasmic effectors, and therefore block the stimulation of downstream cytosolic events (Fig. 6). Whether GTPase activation can occur in the cytosol or active GTPases dissociate from the membrane is unknown. The activation of GTPases in the cytosol is consistent with another recent report[30], but kinetic events have not yet been explored *in vivo*. Integrins stimulate Rac membrane translocation by increasing the affinity of the membranes for Rac[8]. We suggest that this increase occurs at specific sites and enables membranes to compete with Rho-GDI, favouring the displacement of the geranyl geranyl moiety from the Rho-GDI hydrophobic pocket towards the hydrophobic membrane phospholipids. The release of GDI after membrane translocation allows the coupling of activated Rac to effectors, which induces the formation of lamellipodia, thus promoting the extension of the leading edge of the cell. Therefore, growth factors could activate Rac globally in the cell, but integrins would determine the specific local areas where Rac binds to effectors, thus determining where to extend lamellipodia and facilitating efficient cell migration (Fig. 6).

A Rab GDI-displacement factor (GDF), which releases endosomal Rab GTPases from Rab-GDI, was recently identified, and might be involved in localizing Rabs to their correct intracellular compartments[31]. No such factor has yet been identified for the Rho family, but if one exists, it could conceivably participate in the effects described here.

Although local integrin stimulation induces Rac membrane targeting and effector interaction, the FRET signal is not precisely defined around the bead, showing a more diffuse pattern in some cases (Fig. 4). This observation is consistent with the more diffuse FRET signal at cell edges. It could be attributed to a propagation of integrin-initiated binding sites into the surrounding areas, or to diffusion of Rac after membrane translocation has occurred.

Our results suggest that GTP exchange need not be localized for Rac function also to be localized. This concept establishes a major difference with the *Saccharomyces cerevisiae* system, where localization of GEFs to specific sites is required for polarized budding[32], and overexpression of GTPases randomizes the normal budding site pattern[33]. Strikingly, overexpression of V12-Rac or GEFs in mammalian cells can induce migration rather than paralysis[34–36], an observation that is consistent with our model.

In summary, we have determined a mechanism for the spatial regulation of Rho family GTPase function. Constitutively active Rac is diffusely distributed throughout the cell, yet the interaction with a soluble cytoplasmic effector is enhanced at regions of the cell edge or near sites of integrin stimulation. This interaction requires Rac membrane translocation. Rho-GDI, which sequesters Rac in the cytoplasm, blocks effector binding. However, membrane translocation displaces Rho-GDI and allows effectors to bind. Therefore, we have identified an unexpected spatial specificity for Rac–effector interactions and defined a novel function for Rho-GDI. □

Methods

Cell culture and transfections

NIH-3T3 cells were grown in Dulbecco's modified Eagle's Medium (DMEM) supplemented with 10% calf serum, penicillin and streptomycin (GIBCO-BRL, Gaithersberg, MD). Cells were starved for 24 h in 0.2% serum before stimulation and biochemical assays. For suspension, 2×10^6 cells cultured in DMEM containing 0.2% BSA were plated into 15-cm bacterial plastic dishes coated with 10 mg ml^{-1} heat-denatured BSA. For transfections, cells at approximately 50% confluence in 100-mm tissue culture dishes were transfected (1.0 μg total DNA) with the Effectene reagent, according to the manufacturers instructions (Qiagen, San Diego, CA). Expression vector DNAs were supplemented with the proper amounts of the corresponding empty vector. Typically, 0.2 μg of plasmid encoding the various Rho protein mutants and 0.1 μg of pEFBOS-myc–Rho-GDI were transfected in each condition. Unless a GFP–fusion construct was transfected, 0.1 μg of green fluorescent protein vector (Clontech Laboratory Inc, Palo Alto, CA) was routinely included to estimate transfection efficiency, which was consistently around 30%. Cell lysis or fixation and analysis were performed 48 h after transfection, as described for each experiment.

DNA plasmids and constructs

HA-tagged Rac and Cdc42 mutant cDNAs were inserted into the pcDNA3 vector and Myc-tagged Pak–PBD cDNA was inserted in pCMV6, as previously described[14]. Rac effector mutant cDNAs in pRK5 were obtained from A. Hall (London, UK)[12], and pEFBOS-myc–Rho-GDI was obtained from Y. Takai (Osaka, Japan)[37]. The plasmid pCA-GAP–GFP-S65A, containing the membrane-anchoring signal of growth associated protein (GAP)-43 fused to GFP, was obtained from K. Moriyoshi (Kyoto, Japan)[38]. Plasmids encoding GFP-tagged Wt-Rac, Wt-Cdc42, V12-Rac and V12-Cdc42 have been described previously[39]. pRK5-myc–V12-Rac-6Q was kindly provided by J.H. Jackson (La Jolla, CA)[16] and was subcloned in-frame into the *Bam*HI site of pEGP-C1 (Clontech), a mammalian expression vector that adds an N-terminal GFP tag to expressed proteins. pBK-CMV-V12-Rac-C189S (a gift of T. Reid, Amsterdam, The Netherlands) and pRK5-myc–(Q61L–T35S-Rac) were used as templates for PCR-amplification of the mutated Rac inserts that were then subcloned as *Eco*RI-*Bam*HI fragments into pEGFP–C1, to generate GFP–(V12–C189S-Rac) and GFP–(Q61L–T35S-Rac), respectively. All the newly generated constructs were confirmed by DNA sequencing. DNA for microinjections and transfections was purified on caesium gradients.

Purification of recombinant proteins

PBD of human Pak (residues 65–150), with a single cysteine added in the penultimate N-terminal position, was expressed as a C-terminal hexahistidine (His_6) fusion protein from the pET23 vector (Novagen, Madison, WI) and purified from *Escherichia coli*, as described[40]. His_6–PBD was then labelled with Alexa-546–maleimide (Molecular Probes, Eugene, OR), as described[10]. In Rac pull-down assays, PBD was purified as a glutathione *S*-transferase (GST) fusion protein, as previously described[8,41]. Recombinant His_6–N-terminal-tagged human Rho-GDI in a modified pET22B vector was purified from the BL21(DE3) *E. coli* strain, as described[42]. *S. cerevisiae* yeast strain SY1 transformed with the $YepP_{GAL}$–His_6–Rac1–tPMA1 was cultured and lysed to purify recombinant isoprenylated human Rac1, as described[42,43]. Fibronectin was prepared from human plasma, as described[44].

Subcellular fractionation

Adherent and suspended cells were washed, drained and treated with ice-cold hypotonic lysis buffer (10 mM Tris-HCl at pH 7.4, 1.5 mM magnesium chloride, 5 mM potassium chloride, 1 mM dithiothreitol, 0.2 mM sodium vanadate, 1 mM phenyl methylsulphonyl fluoride, 1 μg ml^{-1} aprotinin and 1 μg ml^{-1} leupeptin) for 5 min. Adherent cells were scraped and cell lysates were homogenized with 15 strokes of a Dounce homogenizer. Homogenates were centrifuged at 700*g* for 3 min to pellet nuclei and intact cells. The supernatants were then spun at 40,000*g* for 30 min at 4 °C in a refrigerated centrifuge to sediment particulates. The cytosol-containing supernatant was removed and the crude membrane pellet gently washed with hypotonic lysis buffer. Membrane and cytosol fractions were then assayed for total protein. Equal amounts were analysed by western blotting and quantified by scanning densitometry. Typically, 10 μg of protein was analysed, representing 1–2% of the cytoplasmic fraction and 10–20% of the membrane fraction.

Immunofluorescence microscopy and quantification of the translocation index

Glass coverslips in 24-well plastic dishes were coated overnight with 20 μg ml^{-1} human fibronectin or 1 mg ml^{-1} poly-L-lysine at 4 °C. Dishes were washed three times with PBS, and the fibronectin dishes blocked with 10 mg ml^{-1} heat-denatured BSA. After plating, cells were fixed with 3% paraformaldehyde-PBS for 30 min, permeabilized in 0.2% Triton-X100 in PBS for 5 min, and blocked with 10% normal goat serum. Images were acquired using a BioRad 1024 MRC laser scanning confocal imaging system, and represent the basal *z*-section of the cells in direct contact with the substrate. GFP-positive cells were selected and scored 0 for no detectable GFP in the plasma membrane, 1 for weak GFP plasma membrane staining, and 2 for bright GFP localization in the plasma membrane. The index of translocation to the plasma membrane was calculated as: $(y+2z)/(x+y+z)$, where x, y and z are the number of cells that were scored as 0, 1, or 2, respectively. Each experiment was scored blind independently by two investigators.

Cells for FRET assays and binding to beads

NIH-3T3 cells were grown for 48 h on coverslips in dishes prepared as described[45], and placed in an open chamber with atmospheric and temperature control. Cell nuclei were microinjected with 50 μg ml^{-1} expression vector cDNA, coding for different Rac mutants fused to GFP. After 2 h, cells expressing GFP–Rac were microinjected into the cytoplasm with Alexa–PBD (50 μg ml^{-1}) as described[10,40,46]. After injection, cells were returned to the 37 °C incubator for 30 min, then fixed in 2% formaldehyde for 15 min. Coverslips were rinsed in PBS and mounted onto glass slides with immunomount (ICN, Aurora, OH).

In some cases, after PBD injection cells were incubated for 20 min with 5-μm polystyrene divinylbenzene beads (Duke Scientific Corporation, Palo Alto, CA) at a cell to bead ratio of 1:40. Beads were prepared by washing according to the manufacturer instructions, incubation overnight with 20 μg ml^{-1} fibronectin or 1 mg ml^{-1} poly-L-lysine at 4 °C, and then washing with cold PBS and resuspension by sonication in an ultrasonic bath (Laboratory Supplies Co. Inc, Hicksville, NY). For antibody conjugation, beads were incubated with either 25 μg ml^{-1} rabbit anti-hamster IgG (Sigma Chemicals, St. Louis, MO) and then 10 μg ml^{-1} HMβ1-1 hamster anti-mouse β1 integrin IgG (Pharmingen, San Diego, CA) or 25 μg ml^{-1} goat anti-rat IgG (Sigma), then 10 μg ml^{-1} 5D2-27 rat anti-mouse CD44 IgG (Developmental Studies Hybridoma Bank, The University of Iowa, Iowa City, IA).

Microscopy for FRET assays

Imaging was performed with a BioRad 1024 Confocal Microscope. Filters for these experiments were: (1) GFP–Rac: excitation 488 nm, emission 522 nm; (2) Alexa-546: excitation 568 nm, emission 598 nm; (3) FRET: excitation 488 nm, emission 598 nm. GFP and FRET images were acquired simultaneously and Alexa-546 images were acquired separately at the same plane. Only cells expressing moderate levels of GFP–Rac and Alexa-PBD were studied; high- and low-expressing cells were avoided. GFP and FRET images of cells injected with GFP–Rac only, and Alexa and FRET images of cells injected with Alexa–PBD only, were also obtained in order to determine bleed-through corrections and background corrections, as described[10,40]. The ratio of bleed-through and background correction were then subtracted from the original raw FRET image (8-bit 512 × 512, 0–256 fluorescence intensity range, (arbitrary units)) with Innovision ISEE software (Raleigh, NC). The resultant corrected 8-bit FRET images typically had an average fluorescence intensity range of 0–125. This fluorescence intensity range was displayed using a colour spectrum, where blue was closest to 0 and red closest to 125. Positive FRET in images typically appeared between 63 and 125 (green/yellow to red range). A bead was considered positive when there was an area in the vicinity of the bead scoring a FRET intensity greater than 63, which corresponds to the baseline determined by inactive regions of the cells and by the inactive T35S-Rac mutant. A more quantitative method was employed with cells injected with GFP–V12-Rac and incubated with anti-integrin-β1- or anti-CD44-coated beads. In this case, the integrated FRET value of an area of 500 pixels surrounding the bead was measured and compared between both groups. The average FRET value was calculated by dividing the total FRET intensity of the cell by the cell area in pixels.

Rac pull-down experiments and immunoprecipitation

Rac GTPase assays from whole cells were performed essentially as described[8]. For *in vitro* binding, recombinant isoprenylated human Rac1 purified from yeast was loaded with GDP or GTPγS, as described[47], and 0.5 μg of protein was incubated with different amounts of recombinant purified human Rho-GDI for 30 min at 4° C. Then, 0.5 μg of recombinant human GST–PBD in binding buffer (0.5% NP-40, 50 mM Tris-HCl at pH 7.4, 150 mM sodium chloride, 1 mM magnesium chloride, 1 mM EGTA, 1 mM phenyl methyl sulphonyl fluoride) was added. The PBD was collected on glutathione–agarose beads (Sigma) for 30 min at 4° C, washed and then eluted with SDS sample buffer. Bound Rac was analysed by western blotting with a monoclonal anti-Rac antibody (0.25 μg ml^{-1}; Upstate Biotechnology, Lake Placid, NY). For immunoprecipitation of V12-Rac, lysates of cells transfected with pcDNA3-HA–V12-Rac were precipitated with purified anti-HA 12CA5 monoclonal antibody (10 ng ml^{-1}) before incubation with protein G Sepharose beads (Pharmacia, Uppsala, Sweden), and analysis by western blotting.

RECEIVED 18 OCTOBER 2001; REVISED 4 DECEMBER 2001; ACCEPTED 28 DECEMBER 2001; PUBLISHED 25 FEBRUARY 2002.

1. de Curtis, I. Cell migration: GAPs between membrane traffic and the cytoskeleton. *EMBO Rep.* **2,** 277–281 (2001).
2. Hall, A. Rho GTPases and the actin cytoskeleton. *Science* **279,** 509–514 (1998).
3. Lauffenburger, D. A. & Horwitz, A. F. Cell migration: a physically integrated molecular process. *Cell* **84,** 359–369 (1996).
4. Bishop, A. L. & Hall, A. Rho GTPases and their effector proteins. *Biochem. J.* **348 Pt 2,** 241–255 (2000).
5. Olofsson, B. Rho guanine dissociation inhibitors: pivotal molecules in cellular signalling. *Cell Signal.* **11,** 545–554 (1999).
6. Seabra, M. C. Membrane association and targeting of prenylated Ras-like GTPases. *Cell Signal.* **10,** 167–172 (1998).
7. Keep, N. H. *et al.* A modulator of rho family G proteins, Rho-GDI, binds these G proteins via an immunoglobulin-like domain and a flexible N-terminal arm. *Structure* **5,** 623–633 (1997).
8. del Pozo, M. A., Price, L. S., Alderson, N. B., Ren, X. D. & Schwartz, M. A. Adhesion to the extracellular matrix regulates the coupling of the small GTPase Rac to its effector PAK. *EMBO J.* **19,** 2008–2014 (2000).
9. Symons, M. Adhesion signalling: PAK meets Rac on solid ground. *Curr. Biol.* **10,** R535–R537 (2000).
10. Kraynov, V. S. *et al.* Localized Rac activation dynamics visualized in living cells. *Science* **290,** 333–337 (2000).
11. Dharmawardhane, S., Sanders, L. C., Martin, S. S., Daniels, R. H. & Bokoch, G. M. Localization of p21-Activated Kinase 1 (PAK1) to pinocytic vesicles and cortical actin structures in stimulated cells. *J. Cell Biol.* **138,** 1–14 (1997).
12. Lamarche, N. *et al.* Rac and cdc42 induce actin polymerization and G1 cell cycle progression independently of p65PAK and the JNK/SAPK MAP kinase cascade. *Cell* **87,** 519–529 (1996).
13. Westwick, J. K. *et al.* Rac regulation of transformation, gene expression, and actin organization by multiple, PAK-independent pathways. *Mol. Cell. Biol.* **17,** 1324–1335 (1997).
14. Price, L. S., Leng, J., Schwartz, M. A. & Bokoch, G. M. Activation of rac and cdc42 by integrins mediates cell spreading. *Mol. Biol. Cell* **9,** 1863–1871 (1998).
15. Hancock, J. F., Paterson, H. & Marshall, C. J. A polybasic domain or palmitoylation is required in addition to the CAAX motif to localize p21ras to the plasma membrane. *Cell* **63,** 133–139 (1990).
16. Knaus, U. G., Wang, Y., Reilly, A. M., Warnock, D. & Jackson, J. H. Structural requirements for PAK activation by Rac GTPases. *J. Biol. Chem.* **273,** 21512–21518 (1998).
17. Kozma, R., Ahmed, S., Best, A. & Lim, L. The Ras-related protein Cdc42Hs and bradykinin promote formation of peripheral actin microspikes and filopodia in Swiss 3T3 fibroblasts. *Mol. Cell. Biol.* **15,** 1942–1952 (1995).
18. Jordan, J. D., Landau, E. M. & Iyengar, R. Signalling networks: the origins of cellular multitasking. *Cell* **103,** 193–200 (2000).
19. Teruel, M. N. & Meyer, T. Translocation and reversible localization of signalling proteins: a dynamic future for signal transduction. *Cell* **103,** 181–184 (2000).
20. Kiosses, W. B., Shattil, S. J., Pampori, N. & Schwartz, M. A. Rac recruits high-affinity integrin αvβ3 to lamellipodia in endothelial cell migration. *Nature Cell Biol.* **3,** 316–320 (2001).
21. Miyamoto, S. *et al.* Integrin function: molecular hierarchies of cytoskeletal and signalling proteins. *J. Cell Biol.* **131,** 791–805 (1995).
22. Schwartz, M. A., Lechene, C. & Ingber, D. E. Insoluble fibronectin activates the Na/H antiporter by clustering and immobilizing integrin α5β1, independent of cell shape. *Proc. Natl Acad. Sci. USA* **88,** 7849–7853 (1991).
23. Lewis, J. M. & Schwartz, M. A. Mapping *in vivo* associations of cytoplasmic proteins with integrin β1 cytoplasmic domain mutants. *Mol. Biol. Cell* **6,** 151–160 (1995).
24. Bourguignon, L. Y., Zhu, H., Shao, L. & Chen, Y. W. CD44 interaction with tiam1 promotes Rac1 signalling and hyaluronic acid-mediated breast tumor cell migration. *J. Biol. Chem.* **275,** 1829–1838 (2000).
25. Woods, A. & Couchman, J. R. Syndecan 4 heparan sulfate proteoglycan is a selectively enriched and widespread focal adhesion component. *Mol. Biol. Cell* **5,** 183–192 (1994).
26. Scheffzek, K., Stephan, I., Jensen, O. N., Illenberger, D. & Gierschik, P. The Rac–Rho-GDI complex

and the structural basis for the regulation of Rho proteins by Rho-GDI. *Nature Struct. Biol.* **7,** 122–126 (2000).
27. Hoffman, G. R., Nassar, N. & Cerione, R. A. Structure of the Rho family GTP-binding protein Cdc42 in complex with the multifunctional regulator Rho-GDI. *Cell* **100,** 345–356 (2000).
28. Lian, L. Y. *et al.* Mapping the binding site for the GTP-binding protein Rac-1 on its inhibitor Rho-GDI-1. *Structure Fold Des.* **8,** 47–55 (2000).
29. Longenecker, K. *et al.* How Rho-GDI binds Rho. *Acta Crystallogr. D. Biol. Crystallogr.* **55,** 1503–1515 (1999).
30. Read, P. W. *et al.* Human RhoA/Rho-GDI complex expressed in yeast: GTP exchange is sufficient for translocation of RhoA to liposomes. *Protein Sci.* **9,** 376–386 (2000).
31. Dirac-Svejstrup, A. B., Sumizawa, T. & Pfeffer, S. R. Identification of a GDI displacement factor that releases endosomal Rab GTPases from Rab-GDI. *EMBO J.* **16,** 465–472 (1997).
32. Chant, J. Cell polarity in yeast. *Annu. Rev. Cell Dev. Biol.* **15,** 365–391 (1999).
33. Johnson, D. I. & Pringle, J. R. Molecular characterization of *CDC42*, a *Saccharomyces cerevisiae* gene involved in the development of cell polarity. *J. Cell Biol.* **111,** 143–152 (1990).
34. Leng, J., Klemke, R. L., Reddy, A. C. & Cheresh, D. A. Potentiation of cell migration by adhesion-dependent cooperative signals from the GTPase Rac and Raf kinase. *J. Biol. Chem.* **274,** 37855–37861 (1999).
35. Habets, G. G. *et al.* Identification of an invasion-inducing gene, Tiam-1, that encodes a protein with homology to GDP-GTP exchangers for Rho-like proteins. *Cell* **77,** 537–549 (1994).
36. Michiels, F., Habets, G. G. M., Stam, J. C., vanderKammen, R. A. & Collard, J. G. A function for rac in Tiam1-induced membrane ruffling and invasion. *Nature* **375,** 338–340 (1995).
37. Fukumoto, Y. *et al.* Molecular cloning and characterization of a novel type of regulatory protein (GDI) for the rho proteins, ras p21-like small GTP-binding proteins. *Oncogene* **5,** 1321–1328 (1990).
38. Moriyoshi, K., Richards, L. J., Akazawa, C., O'Leary, D. D. & Nakanishi, S. Labeling neural cells using adenoviral gene transfer of membrane- targeted GFP. *Neuron* **16,** 255–260 (1996).
39. del Pozo, M. A., Vicente-Manzanares, M., Tejedor, R., Serrador, J. M. & Sanchez-Madrid, F. Rho GTPases control migration and polarization of adhesion molecules and cytoskeletal ERM components in T lymphocytes. *Eur. J. Immunol.* **29,** 3609–3620 (1999).
40. Chamberlain, C. E., Kraynov, V. S. & Hahn, K. M. Imaging spatiotemporal dynamics of Rac activation *in vivo* with FLAIR. *Methods Enzymol.* **325,** 389–400 (2000).
41. Glaven, J. A., Whitehead, I., Bagrodia, S., Kay, R. & Cerione, R. A. The Dbl-related protein, Lfc, localizes to microtubules and mediates the activation of Rac signalling pathways in cells. *J. Biol. Chem.* **274,** 2279–2285 (1999).
42. Gong, M. C. *et al.* Regulation by GDI of RhoA/Rho-kinase-induced Ca2+ sensitization of smooth muscle myosin II. *Am. J. Physiol. Cell Physiol.* **281,** C257–C269 (2001).
43. Read, P. W. & Nakamoto, R. K. Expression and purification of Rho/Rho-GDI complexes. *Methods Enzymol.* **325,** 15–25 (2000).
44. Renshaw, M. W., Ren, X.-D. & Schwartz, M. A. Growth factor activation of MAP kinase requires cell adhesion. *EMBO J.* **16,** 5592–5599 (1997).
45. Kiosses, W. B., Daniels, R. H., Otey, C., Bokoch, G. M. & Schwartz, M. A. A function for p21-activated kinase in endothelial cell migration. *J. Cell. Biol.* **147,** 831–844 (1999).
46. Chamberlain, C. & Hahn, K. M. Watching proteins in the wild: fluorescence methods to study protein dynamics in living cells. *Traffic* **1,** 755–762 (2000).
47. Chong, L. D., Traynor-Kaplan, A., Bokoch, G. M. & Schwartz, M. A. The small GTP-binding protein Rho regulates a phosphatidylinositol 4-phosphate 5-kinase in mammalian cells. *Cell* **79,** 507–513 (1994).

ACKNOWLEDGEMENTS

We thank P. Read for providing plasmids for purification of Rho-GDI and prenylated Rac, A. Hall for Rac effector mutants, Y. Takai for pEFBOS-myc–Rho-GDI, J.H. Jackson for pRK5-myc–V12-Rac-6Q, K. Moriyoshi for the GAP-43–GFP plasmid and A. Woods for the 150.9 monoclonal anti-syndecan-4. We also thank C. Chamberlain for technical advice establishing the FRET assays, and S. Shattil and E. Tzima for their critical comments. This work was supported by United States Public Health Service grant RO1 GM47214 (to M.A.S) and GM39434 (to K.M.H). M.A.d.P. was supported by the Human Frontier Science Program (LT0019/1998-M) and then by a Lady Tata Memorial Trust International Award for Research in Leukemia.

Correspondence and request for material should be addressed to M.A.S. or M.A.D.P.

Supplementary Information is available on *Nature Cell Biology's* website (http://cellbio.nature.com).

COMPETING FINANCIAL INTERESTS

The authors declare that they have no competing financial interests.